J Mater Sci (2009) 44:433–440
DOI 10.1007/s10853-008-3135-7

Wear resistance of electrodeposited Ni–B and Ni–B–Si_3N_4 composite coatings

K. Krishnaveni · T. S. N. Sankara Narayanan · S. K. Seshadri

Received: 28 August 2008 / Accepted: 24 November 2008 / Published online: 11 December 2008

Abstract The wear resistance of electrodeposited (ED) Ni–B and Ni–B–Si_3N_4 composite coatings is compared. The effect of incorporation of Si_3N_4 particles in the ED Ni–B matrix on the surface morphology, structural characteristics and microhardness has been evaluated to correlate the wear resistance. The wear mechanism of ED Ni–B and Ni–B–Si_3N_4 composite coatings appears to be similar; both involve intensive plastic deformation of the coating due to the ploughing action of the hard counter disc. However, the extent of wear damage is relatively small for ED Ni–B–Si_3N_4 composite coatings.

Introduction

The idea of codepositing various second phase particles in electrodeposited (ED) and electroless (EL)-deposited metal matrix and thereby taking advantage of their desirable qualities, such as high hardness, excellent wear and abrasion resistance and improved corrosion resistance, has led to the development of composite coatings with a wide range of possible combination and properties [1–6]. A number of oxides, carbides and nitrides were used as second phase particles to produce ED or EL composite coatings. Silicon nitride (Si_3N_4) is a very hard ceramic material, which retains its room temperature strength up to 1200 °C and possesses excellent dimensional stability and oxidation resistance. The Si_3N_4 particles were successfully codeposited in ED Ni, ED Ni–P, ED Ni–Co and EL Ni–P matrix by dispersing them in the respective plating baths [6–14]. Codeposition of Si_3N_4 particles in ED Ni matrix is also possible by brush plating technique [15]. The incorporation of Si_3N_4 particles in ED or EL Ni or Ni alloy matrix enables an increase in the hardness and improvement in the tribological behaviour [6–14]. The use of ED and EL Ni–P–Si_3N_4 composite coating has also been explored for a variety of industrial components [8, 11]. Wang and Tung [8] have studied the scuffing and wear behaviour of ED Ni–P–Si_3N_4 composite-coated aluminium piston skirt rubbing against an aluminium cylinder bore. According to them, ED Ni–P–Si_3N_4 composite-coated aluminium piston skirts offer moderate scuffing and wear resistance. Das et al. [11] have studied the formation and characteristics of EL Ni–P–Si_3N_4 composite coating on SAE 52100 bearing steel. Based on the significant improvement in wear resistance obtained under water lubricated conditions, they recommend the use of such coatings for ferrous-based bearings for water lubricated applications. However, it is important to note that the metal matrix in which the second phase particles are incorporated also plays a vital role in achieving the desired performance. Xinmin and Zonggang [16] have suggested that the metal matrix should be capable of supporting the second phase particle to achieve superior wear resistance, both in as-plated and heat-treated conditions. Both ED and EL Ni–B alloy matrix possess high hardness and superior wear resistance [17–19]. Hence, they can be considered as an ideal choice for the incorporation of second phase particles. Studies on ED and EL Ni–B-based composite coatings are rather limited. The formation and characteristics of ED Ni–B–Si_3N_4 composite coating was reported in our earlier

K. Krishnaveni · T. S. N. Sankara Narayanan (✉)
National Metallurgical Laboratory (Madras Centre),
CSIR Complex, Taramani, Chennai 600113, India
e-mail: tsnsn@rediffmail.com

S. K. Seshadri
Department of Metallurgical and Materials Engineering,
Indian Institute of Technology, Chennai 600036, India

article [20]. This article aims to study the wear resistance of ED Ni–B–Si_3N_4 composite coating and to compare its ability with ED Ni–B coating.

Experimental

Mild steel discs (30-mm diameter and 5-mm thick), mild steel pins (10-mm diameter and 50-mm length) and copper sheets (electrolytic grade; 1-mm thick) were used as the substrate material for the electrodeposition of Ni–B and Ni–B–Si_3N_4 composite coatings. Copper sheet was used to evaluate the plating rate and structural characteristics; mild steel discs were used to evaluate the hardness and surface morphology, whereas mild steel pins were used to evaluate the wear resistance. The details of surface preparation and electrodeposition of Ni–B and Ni–B–Si_3N_4 composite coatings were already presented in our earlier articles [17, 20]. The chemical composition of the plating bath and its operating conditions are listed in Table 1. The Si_3N_4 particles have diameters d_{10}, d_{50} and d_{80} of 0.08, 0.39 and 0.92 μm, respectively, with a mean diameter of 0.80 μm. The details of the chemical analysis of nickel, boron and the determination of level of incorporation of Si_3N_4 particles in the ED Ni–B matrix were already given in our earlier articles [17, 20]. The structure of ED Ni–B and Ni–B–Si_3N_4 composite coatings, both in as-plated and heat-treated conditions, was determined by X-ray diffraction (XRD) measurements using Cu Kα ($\lambda = 1.5418$ Å) radiation. The surface morphology of these coating was assessed by a scanning electron microscope (SEM). The microhardness of these coatings (thickness: 20 μm), both in as-plated as well as heat-treated (200, 300, 400, 500, 600 °C for 1 h) conditions, was measured on the surface using a Leica microhardness tester with a Vickers diamond indenter under a load of 100 g (0.98 N). The lap time for each indentation was 15 s and the values reported represent the average of five measurements.

Table 1 Bath composition and operating conditions used to prepare ED Ni–B–Si_3N_4 composite coatings

Bath composition	
Nickel sulphate hexahydrate (g/L)	240
Nickel chloride hexahydrate (g/L)	45
Boric acid (g/L)	30
Dimethylamine borane (g/L)	3
Si_3N_4 powder (g/L)	50
Operating conditions	
Temperature	45 ± 1 °C
pH	3.5
Current density	1 A/dm^2
Agitation	Mechanical—using magnetic stirrer at 600 rpm
Time	100 min

The wear resistance of ED Ni–B and Ni–B–Si_3N_4 composite-coated mild steel pins, both in as-plated and heat-treated conditions, was evaluated using a pin-on-disc apparatus (DUCOM, India). Steel discs (composition conforming to EN 31 specification) of 10-cm diameter and 5-mm thickness, fully hardened (R_c 63) and surface ground to a finish (R_a) of 0.02 μm, were chosen as counter face materials. The applied normal loads were 8, 10 and 12 N. The sliding speed was kept constant at 0.5 m/s for all the tests by adjusting the diameter of the wear track and the rotational speed of the disc. The coatings used for wear resistance studies have a thickness of 20 μm. After the wear tests, the pins were cleaned in acetone in an ultrasonic bath for about 10 min to remove the loose particles and wear debris from the surface. The loss in weight due to wear was calculated by weighing the pins before and after each test on a balance with an accuracy up to 0.1 mg. Three tests were done for each load condition. The specific wear rate was calculated by the expression:

$$w_s = w/(lL)$$

where w is the wear mass, L the normal load and l is the sliding distance. The sliding distance was calculated at the mean radius of the disc. Immediately after the end of each test, the wear track pattern on the pins was examined using SEM. The roughness of the pins, before and after wear test, was determined using a portable roughness measuring station (Make: Mahr; Model: Perthometer-M2).

Results and discussion

Characteristics of ED Ni–B and Ni–B–Si_3N_4 composite coatings

The plating rate of ED Ni–B and Ni–B–Si_3N_4 composite coatings is about 12 μm/h. The incorporation of Si_3N_4 particles in the ED Ni–B matrix causes a decrease in metallic lustre, increase in surface roughness and change in chemical composition. The average surface roughness (R_a) of ED Ni–B–Si_3N_4 composite coatings is 1.17 μm. The chemical composition of coating changes from 97 wt% Ni and 3 wt% B to 89.6 wt% Ni; 2.4 wt% B and 8 wt% Si_3N_4 with the incorporation of Si_3N_4 particles in the ED Ni–B matrix. The surface morphology of ED Ni–B and Ni–B–Si_3N_4 composite coatings is shown in Fig. 1a and b, respectively. ED Ni–B coatings reveal the formation of well-crystallized, uniform and fine-grained deposits, with some cracks that are emerged due to the stress in the coatings (Fig. 1a). The ED Ni–B–Si_3N_4 composite coatings consist of a homogeneous fine globular structure in which

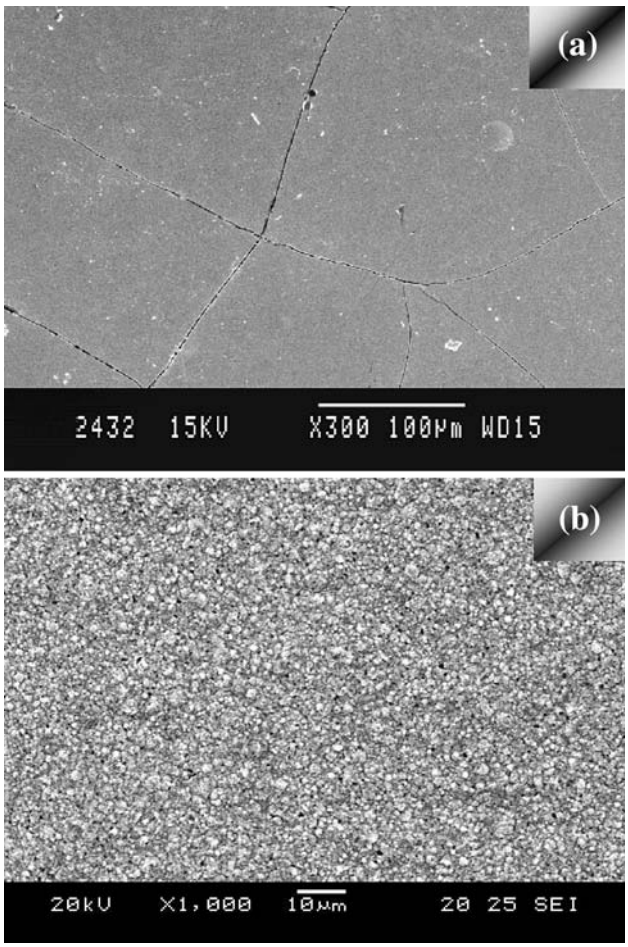

Fig. 1 SEMs of **a** ED Ni–B coating; **b** ED Ni–B–Si_3N_4 composite coating

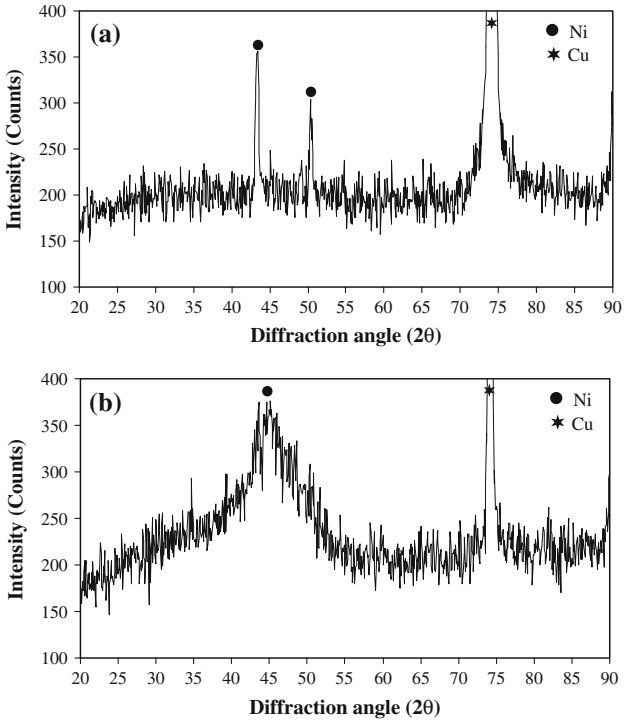

Fig. 2 XRD patterns of as-plated **a** ED Ni–B coating; **b** ED Ni–B–Si_3N_4 composite coating

the Si_3N_4 particles are uniformly distributed throughout the matrix (Fig. 1b). The XRD patterns of as-plated ED Ni–B and Ni–B–Si_3N_4 composite coatings are shown in Fig. 2a and b, respectively. The XRD pattern of as-plated ED Ni–B coating indicates that the nucleation of the nickel phase in not completely prevented since the boron concentration is relatively low. Alloying of boron with nickel causes a change in the preferred orientation of the Ni–B coating with Ni (111) being the most intense reflection. Wu and Sha [21] have also observed Cu (111) as the preferred orientation in EL-deposited copper coatings. The reason for the change in the preferred orientation of ED Ni–B coating has already been discussed in our earlier article [17]. It is evident from Fig. 2b that the incorporation of Si_3N_4 particles causes a significant change in the structure of the ED Ni–B–Si_3N_4 composite coatings. The absence of the reflection from Ni (200) plane and the change in intensity and broadening of the reflection from Ni (111) plane at higher particle loadings suggest a change in crystal orientation of the coating following incorporation of the Si_3N_4 particles in the ED Ni–B matrix. The influence of incorporation of second phase particles on the crystal orientation of electro- and EL-deposited composite coatings has been studied by many researchers [22–25]. Qu et al. [25] have reported that though the incorporation of CeO_2 particles in ED Ni matrix does not change the preferred orientation of Ni (200), it causes a significant increase in the relative intensities of reflections of Ni (111) and Ni (220) orientations. An increase in the intensity of reflection of Cu (111) orientation is also observed by Wu and Sha [21] on EL copper deposits, which is attributed to the presence of excess amount of copper (111) planes parallel to the surface. The increase in the intensity of reflection of the Ni (111) orientation of ED Ni–B–Si_3N_4 composite coating with the incorporation of Si_3N_4 particles in the ED Ni–B matrix could be also due to the formation of excess amount of Ni (111) plane. The grain size of as-plated ED Ni–B and Ni–B–Si_3N_4 composite coating is 10–13 and 6–8 nm, respectively. The XRD patterns of ED Ni–B and Ni–B–Si_3N_4 composite coatings after the heat-treatment at 400 °C for 1 h are shown in Fig. 3a and b, respectively. It is evident from Fig. 3 that heat-treatment increases the crystallinity of these coatings and enables the formation of Ni_3B phase. The Ni (111) texture is retained even after heat-treatment. The intensity of the reflection from Ni (111) plane of ED Ni–B–Si_3N_4 composite coating is relatively higher than that of ED Ni–B coating, which further confirms the change in crystal orientation following the

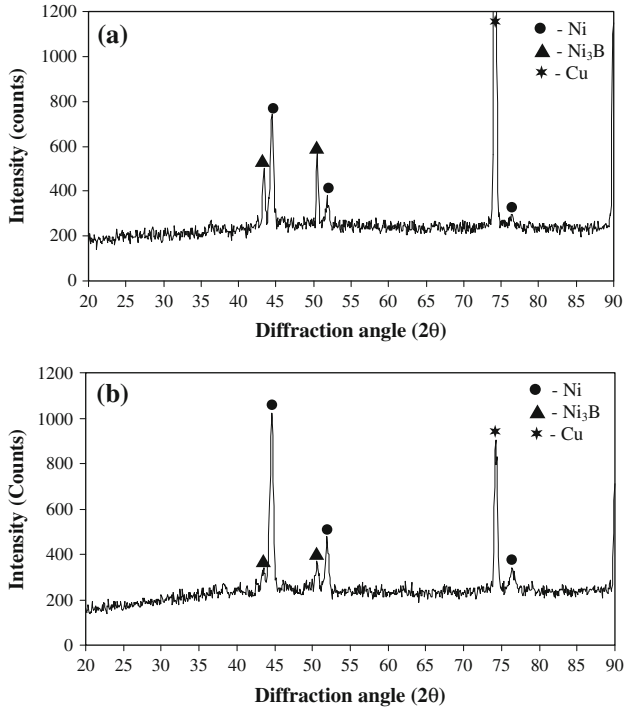

Fig. 3 XRD patterns of **a** ED Ni–B coating; **b** ED Ni–B–Si_3N_4 composite coatings after heat-treatment at 400 °C for 1 h

incorporation of Si_3N_4 particles in the ED Ni–B matrix. Heat-treatment increases the grain size of both ED Ni–B and Ni–B–Si_3N_4 composite coatings. After heat-treatment at 400 °C for 1 h, the grain size of ED Ni–B and Ni–B–Si_3N_4 composite coatings are increased to 17–20 and 12–14 nm, respectively.

Microhardness of ED Ni–B and Ni–B–Si_3N_4 composite coating

The microhardness of as-plated ED Ni–B and Ni–B–Si_3N_4 composite coatings is 609 ± 15 and 640 ± 16 $HV_{0.1}$, respectively, which is considerably high compared with that of bulk Ni (100–150 $HV_{0.1}$) and ED Ni (250–350 $HV_{0.1}$). The hardness of ED Ni–B coating is relatively higher than that of EL Ni high-P coatings, in their as-plated condition [6, 26]. The increase in hardness of the ED Ni–B–Si_3N_4 composite coating compared with its plain counterpart can be ascribed to the combined strengthening effect, primarily the dispersion hardening and, to some extent the solid solution hardening. However, the hardness of ED Ni–B–Si_3N_4 composite coating is relatively lower than that of EL Ni–P–Si_3N_4 composite coating (720 ± 12 $HV_{0.1}$) having a similar level of incorporation of Si_3N_4 particles, of 8 wt%, suggesting that the influence of the matrix is also an important factor in deciding the hardness of composite coatings. The effect of heat-treatment temperature on the hardness of ED Ni–B and Ni–B–Si_3N_4 composite coatings is shown in Fig. 4. There is a marginal increase in hardness of these coatings when the heat-treatment temperature is increased to 200 °C. With further increase in temperature, however, the hardness increases rapidly, as the structure of the coating matrix begins to change. The hardness versus heat-treatment temperature curve resembles that of a bell shape with its maximum at 400 °C in both cases. The hardness of ED Ni–B and Ni–B–Si_3N_4 composite coatings, after heat-treatment at 400 °C for 1 h, is 817 ± 22 and 955 ± 24 $HV_{0.1}$, respectively. Beyond 400 °C, the hardness of these coatings starts to decrease. The increase in hardness with increase in heat-treatment temperature up to 400 °C is due to the precipitation of nickel boride (Ni_3B), which is confirmed by XRD [17, 20]. Beyond 400 °C, the ED Ni–B matrix begins to soften as a result of coarsening of the Ni_3B particles, which thereby reduces the number of hardening sites. A similar behaviour of change in hardness with heat-treatment temperature was observed before for ED and EL Ni–P and Ni–B coatings and their composite counterparts [6, 7, 13, 14, 17–19, 26]. The hardness of ED Ni–B and Ni–B–Si_3N_4 composite coatings, after heat-treatment at 400 °C for 1 h, is relatively lower than that of EL Ni–11 wt% P (980 ± 15 $HV_{0.1}$) and EL Ni–10.1 wt% P–8.10 wt% Si_3N_4 composite coatings (1171 ± 14 $HV_{0.1}$) [6]. This can be explained due to the formation of higher volume fraction of nickel phosphide phases in EL Ni–P and Ni–P–Si_3N_4 composite coatings compared with that of the nickel boride phases that would form in ED Ni–B and Ni-B-Si_3N_4 composite coatings, after heat-treatment at 400 °C for 1 h.

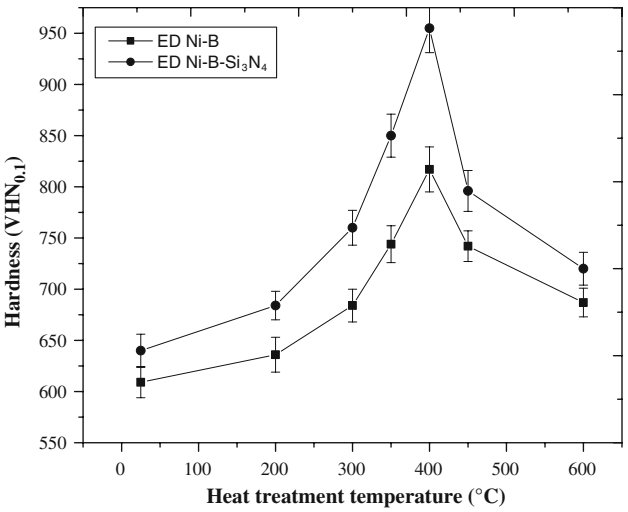

Fig. 4 Variation in hardness of ED Ni–B and Ni–B–Si_3N_4 coatings as a function of heat-treatment temperature

The concept of kinetic strength analysis, which was first proposed in 1945 by Hollomon and Jaffe from their work on time–temperature relations in tempering steel [27] and subsequently used by different authors for investigating the

directional recrystallization of superalloys [28, 29], hardening of steels [30] and structure and hardening in welds [31], was used by Keong et al. [26] to analyse the relationship between the increased hardening effect and the kinetic energy 'Q' of the effect at isothermal treatment for EL Ni–P coating. Keong et al. [26] have studied the effectiveness of adopting kinetic strength concept, to describe the increased hardening effect in EL Ni–P-coated samples, by performing a linear regression analysis of the plot between $\ln(\Delta H)$ vs $1000/R_gT_K$, where ΔH is the increment in hardness of the coating with increase in temperature, R_g the gas (Boltzmann) constant and T_K is the heat-treatment temperature in Kelvin. The slope of the plot provides a measure of the kinetic energy, Q. The applicability of the concept of kinetic strength analysis for ED Ni–B and Ni–B–Si_3N_4 composite coatings is studied using the hardness data obtained as a function of heat-treatment temperature. The calculation of the kinetic parameters using the hardness data is listed in Table 2. The plot of $\ln(\Delta H)$ vs $1000/R_gT_K$ made using the data points (636–817 $VHN_{0.1}$ for ED Ni–B and from 684 to 955 $VHN_{0.1}$ for Ni–B–Si_3N_4 composite coatings) corresponding to the increasing hardening effect is shown in Fig. 5. The slope of the lines represents the activation energy of increased hardening that is $Q = 11.55$ and 13.13 kJ/mol for ED Ni–B and Ni–B–Si_3N_4 composite coatings, respectively. The correlation coefficient values ($R^2 = 0.9999$ for ED Ni–B and 0.998 for ED Ni–B–Si_3N_4) suggest that the result of kinetic modelling has been satisfactory for ED Ni–B and Ni–B–Si_3N_4 composite coatings. A satisfactory fit was obtained before Keong et al. [26] for the data obtained in a previous literature report and for some of their data.

Table 2 Calculation of kinetics parameters using the Vickers hardness data of ED Ni–B and Ni–B–Si_3N_4 composite coatings

Temperature (T)[a] (°C)	Hardness (H) ($VHN_{0.1}$)	ΔH	$1000/R_gT_K$[b]	$\ln(\Delta H)$
ED Ni–B coating				
25	609	0	–	–
200	636	27	0.2543	3.2958
300	684	48	0.2099	3.8712
350	744	60	0.1931	4.0943
400	817	73	0.1787	4.2905
ED Ni–B–Si_3N_4 composite coating				
25	640	0	–	–
200	684	44	0.2543	3.7842
300	760	76	0.2099	4.3307
350	850	90	0.1931	4.4998
400	955	105	0.1787	4.6539

[a] Isothermal heating temperature (for 1-h period)

[b] Temperature in unit Kelvin (K)

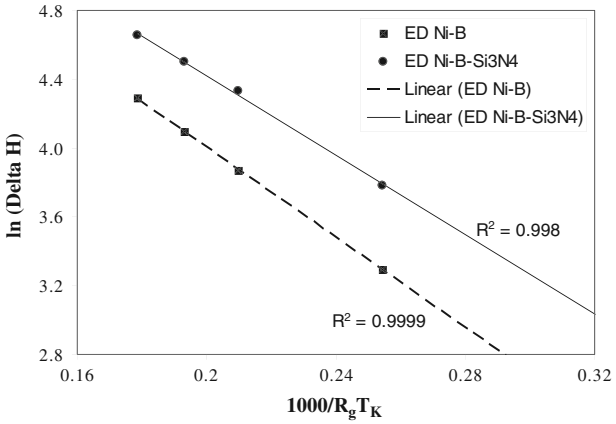

Fig. 5 Plot of $\ln(\Delta H)$ vs $1000/R_gT_K$ using the Vickers hardness ($HV_{0.1}$) data of ED Ni–B and Ni–B–Si_3N_4 composite coatings

According to Keong et al. [26], the concept of kinetic strength analysis could be used to provide approximations for the kinetic interpretation of increased hardening effects for EL Ni–P-coated samples, provided that such effects do not involve stages with very different kinetic energies. The better linear fit observed for ED Ni–B and Ni–B–Si_3N_4 composite coatings suggests the applicability of kinetic strength analysis and confirms that this concept can be used for studying the relation between the increased hardening effect and the kinetic energy Q of the effect at isothermal treatment for ED Ni–B coatings and their composite counterparts.

Wear resistance of ED Ni–B and Ni–B–Si_3N_4 composite coating

The wear resistance of ED Ni–B and Ni–B–Si_3N_4 composite coatings, both in as-plated and heat-treated (400 °C for 1 h) conditions, is studied using three different applied normal loads, namely, 8, 10 and 12 N. The specific wear rate is a measure of the ability of the coating to offer wear resistance against the hard counterface material (hardened steel of EN 31). The specific wear rate of ED Ni–B and Ni–B–Si_3N_4 composite coatings, calculated using the loss in weight due to wear, is listed in Table 3. The increase in specific wear rate of both types of coatings with increase in applied normal load indicates a decrease in wear resistance at higher applied loads and this trend is common for both as-plated and heat-treated ED Ni–B and Ni–B–Si_3N_4 composite coatings. The specific wear rate of ED Ni–B–Si_3N_4 composite coating is lower than that of ED Ni–B coating, both in as-plated and heat-treated conditions. Improvement in wear resistance following incorporation of hard second phase particles in electro- and EL nickel matrix has also been observed by several researchers [6, 7, 32, 33]. The improvement in wear resistance offered by ED

Table 3 Specific wear rate and average coefficient of friction of ED Ni–B and Ni–B–Si_3N_4 composite coating in their as-plated and heat-treated conditions obtained at different applied loads after a sliding distance of 1800 m

Applied load (N)	Specific wear rate[a] (kg/N/m × 10^{-10})				Average coefficient of friction[a] (μ_{av})			
	As-plated		Heat-treated at 400 °C/h		As-plated		Heat-treated at 400 °C/h	
	ED Ni–B	ED Ni–B–Si_3N_4	ED Ni–B	ED Ni–B–Si_3N_4	ED Ni–B	ED Ni–B–Si_3N_4	ED Ni–B	ED Ni–B–Si_3N_4
8	6.41	5.32	4.89	3.53	0.65	0.69	0.61	0.63
10	7.30	6.21	5.97	4.43	0.67	0.73	0.64	0.67
12	8.44	7.12	7.14	5.56	0.69	0.78	0.66	0.70

[a] Average of three determinations

Ni–B–Si_3N_4 composite coating compared with that of ED Ni–B coating is due to (i) the characteristics of the Si_3N_4 particles, such as high hardness and high resistance to plastic deformation, which is superior to that of ED Ni–B alloy matrix; and (ii) the dispersion of the Si_3N_4 particles in the ED Ni–B matrix. The uniform distribution of Si_3N_4 particles in the ED Ni–B matrix (Fig. 1) could act as supporting points, strengthening the ED Ni–B alloy matrix and enables an improvement in wear resistance. Similar observations were made in the past by many researchers [7, 34–36].

At all the applied loads, the specific wear rate is lower for heat-treated ED Ni–B and Ni–B–Si_3N_4 composite coatings compared with that obtained for the as-plated ones. This is due to the formation of hard nickel boride phases following heat-treatment [17, 20], which presents a virtually incompatible surface for the counterface material, as there could be very little solubility between iron and these hard nickel boride phases, leading to a decrease in specific wear rate of heat-treated coatings. Besides, following heat treatment, the hardness of ED Ni–B–Si_3N_4 composite coatings is increased following the incorporation of Si_3N_4 particles in the ED Ni–B matrix. The ED Ni–B–Si_3N_4 composite coatings have a double strengthening effect—dispersion strengthening of the hard Si_3N_4 particles and precipitation strengthening of the ED Ni–B alloy matrix. Hence, when the counterface material comes in contact with the ED Ni–B–Si_3N_4 composite matrix, the high hardness of the later enables it to have lower wear.

The average friction coefficient, μ_{av}, of ED Ni–B and Ni–B–Si_3N_4 composite coatings in as-plated and heat-treated conditions, is listed in Table 3. The friction coefficient of ED Ni–B–Si_3N_4 composite coatings is relatively high compared with ED Ni–B coating due to their high surface roughness and high mechanical interlocking forces under similar loading and temperature conditions. Similar observations were made before by Wu et al. [35] and Grosjean et al. [37]. According to Grosjean et al. [37], the gradual increase in friction coefficient is due to the high hardness and abrasive properties of the second phase particles. The coefficient of friction of heat-treated ED Ni–B and Ni–B–Si_3N_4 composite coatings are lower compared with their as-plated counterparts. As already mentioned, this is due to the ability of heat-treated ED Ni–B and Ni–B–Si_3N_4 coating matrix to present a virtually incompatible surface for the hard counterface material. Besides, the build up of iron oxides at the interface could act as a lubricant film and enables a decrease in the coefficient of friction in heat-treated coatings.

The mechanism of wear of ED Ni–B and Ni–B–Si_3N_4 composite coatings depends on the attractive force between the atoms of nickel from the coating and iron from the counter disc. Adhesive wear is most likely to occur under the present experimental conditions which induce a substantial attractive force between these mating surfaces, leading to a high mutual solubility of nickel and iron. The SEMs of the wear track pattern of as-plated ED Ni–B and Ni–B–Si_3N_4 composite coatings are shown in Fig. 6a and b, respectively. Severe shearing of the surface layers of the coating due to the ploughing action of the hard counter disc (hardened steel of EN 31) is clearly evident [38, 39]. This type of morphological feature, commonly called “prows”, is reported for adhesive wear failure of EL Ni–P and Ni–B coatings [6, 19]. The transferred patches from ED Ni–B and Ni–B–Si_3N_4 composite coatings and the wear debris present on the surface of the counter disc clearly indicate the occurrence of adhesion between them, which is further supported by the high mutual solubility of nickel and iron. Hence, adhesive wear appears to be the most likely mechanism of ED Ni–B and Ni–B–Si_3N_4 composite coatings in their as-plated condition.

In contrast to the as-deposited coatings, heat-treated coatings exhibit a bright and smooth finish with fine grooves along the sliding direction (Fig. 6c, d). The loose debris generated during the wear process gets displaced to the sides leading to the formation of grooves along the wear track. In a substantial portion of the wear tracks, no gross adhesion between the coated pins and the counter disc is observed. In support of the morphological features of the wear track pattern, the R_a value is relatively low for heat-treated ED Ni–B and Ni–B–Si_3N_4 composite coatings. The R_a value of ED Ni–B and Ni–B–Si_3N_4 composite

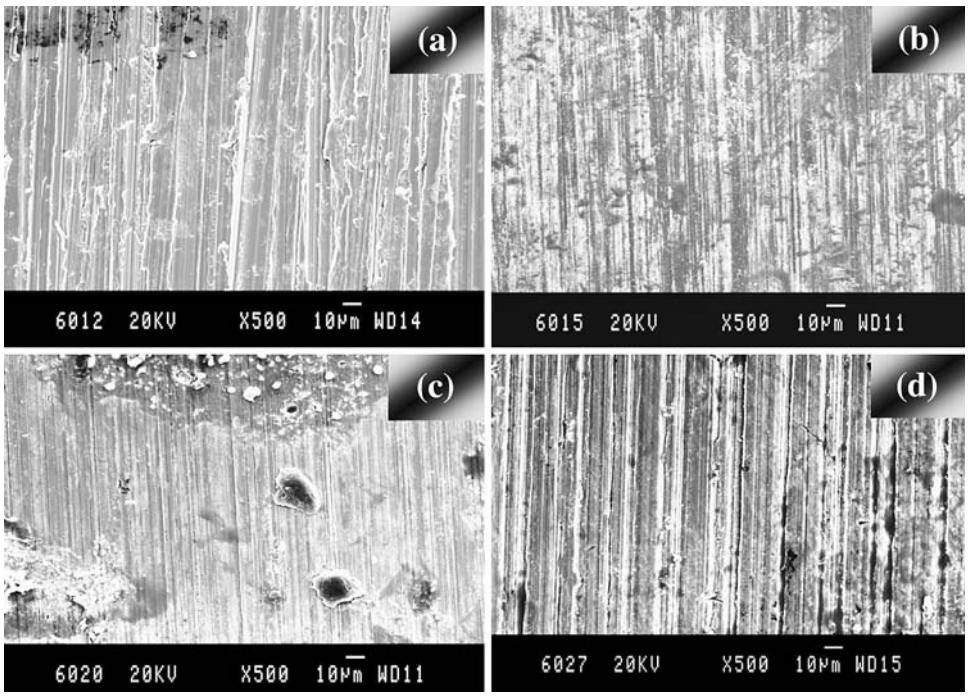

Fig. 6 Wear track patterns of ED Ni–B (**a**, **c**) and Ni–B–Si_3N_4 composite coatings (**b**, **d**) in their as-plated and heat-treated conditions: **a**, **b** As-plated; **c**, **d** heat-treated at 400 °C for 1 h. (Applied load: 10 N; sliding distance: 1800 m.)

coating after wear testing at a load of 12 N are 0.55 and 0.32 μm, respectively, in as-plated and 0.25 and 0.18 μm, respectively, in heat-treated conditions. The relatively low R_a value obtained for heat-treated coatings compared with the as-plated ones is due to the increase in hardness, leading to glazing of these deposits against the counterface material and strongly support the above wear mechanism suggested for heat-treated coatings.

Conclusions

The incorporation of Si_3N_4 particles in the ED Ni–B matrix decreases the metallic lustre, increases the surface roughness and changes the chemical composition. The average surface roughness (R_a) of the ED Ni–B–Si_3N_4 composite coating is 1.17 μm. The chemical composition of coating changes from 97 wt% Ni and 3 wt% B to 89.6 wt% Ni; 2.4 wt% B and 8 wt% Si_3N_4 with the incorporation of Si_3N_4 particles in the ED Ni–B matrix. The surface morphology of the ED Ni–B coatings reveals the formation of well-crystallized, uniform and fine-grained deposits, whereas the ED Ni–B–Si_3N_4 composite coatings consist of a homogeneous fine globular structure in which the Si_3N_4 particles are uniformly distributed throughout the matrix. Incorporation of Si_3N_4 particles in the ED Ni–B matrix causes a change in crystal orientation. Heat-treatment (400 °C for 1 h) increases the crystallinity of these coatings and enables the formation of Ni_3B phase. The microhardness of the as-plated coatings is increased from 609 ± 15 to 640 ± 16 $HV_{0.1}$, following the incorporation of 8 wt% Si_3N_4 particles in the ED Ni–B matrix. The increase in hardness of the ED Ni–B–Si_3N_4 composite coating compared with its plain counterpart can be ascribed to the combined strengthening effect, primarily due to the dispersion hardening induced by the Si_3N_4 particles and to some extent the solid solution hardening of the matrix contributes to the increase in hardness. Heat-treatment (400 °C for 1 h) increases the hardness of ED Ni–B and Ni–B–Si_3N_4 composite coatings to 817 ± 22 and 955 ± 24 $HV_{0.1}$, respectively. The increase in hardness of these coatings after heat-treatment is due to the precipitation of nickel boride (Ni_3B). Beyond 400 °C, the hardness of these coatings starts to decrease due to softening of the matrix following coarsening of the Ni_3B particles. The applicability of the concept of kinetic strength analysis for ED Ni–B and Ni–B–Si_3N_4 composite coatings is verified using the hardness data obtained as a function of heat-treatment temperature. The results of the study confirm that the concept of kinetic strength analysis can be used to study the relation between the increased hardening effect and the kinetic energy Q of the effect at isothermal treatment for ED Ni–B coatings and their composite counterparts. The wear resistance of ED Ni–B–Si_3N_4 composite coatings is higher than that of ED Ni–B coatings, both in as-plated and heat-treated conditions. The wear mechanism of ED Ni–B–Si_3N_4 composite coatings is similar to that of ED Ni–B coatings—intensive plastic deformation of the coating due to the ploughing action of the hard counter disc. However, the extent of wear damage is smaller for ED Ni–B–Si_3N_4 composite coatings.

Acknowledgements Financial support given to this study by the Council of Scientific and Industrial Research (CSIR), New Delhi, India, was gratefully acknowledged. The authors are thankful to Prof. S. P. Mehrotra, Director, National Metallurgical Laboratory, Jamshedpur, for his constant support and encouragement to carry out this research work.

References

1. Musiani M (2000) Electrochim Acta 45:3397
2. Agarwala RC, Agarwala V (2003) Sadhana 28:475
3. Balaraju JN, Sankara Narayanan TSN, Seshadri SK (2003) J Appl Electrochem 33:807
4. Low CTJ, Wills RGA, Walsh FC (2006) Surf Coat Technol 201:371
5. Sarret M, Müller C, Amell A (2006) Surf Coat Technol 201:389
6. Balaraju JN (2000) PhD Thesis, Indian Institute of Technology-Madras, Chennai
7. Ramesh CS, Seshadri SK (2003) Wear 255:893
8. Wang Y, Tung SC (1999) Wear 225–229:1100
9. Xia Y, Sasaki S, Murakami T, Nakano M, Shi L, Wang H (2007) Wear 262:765
10. Shi L, Sun CF, Zhou F, Liu WM (2005) Mater Sci Eng A 397:190
11. Das CM, Limaye PK, Grover AK, Suri AK (2007) J Alloys Compd 436:328
12. Balaraju JN, Sankara Narayanan TSN, Seshadri SK (2006) Mater Res Bull 41(4):847
13. Balaraju JN, Rajam KS (2007) Int J Electrochem Sci 2:747
14. Balaraju JN, Rajam KS (2008) J Alloys Compd 459:311
15. Du L, Xu B, Dong S, Yang H, Tu W (2004) Wear 257:1058
16. Xinmin H, Zonggang D (1993) Plat Surf Finish 80:62
17. Krishnaveni K, Sankara Narayanan TSN, Seshadri SK (2006) Mater Chem Phys 99:300
18. Sankara Narayanan TSN, Seshadri SK (2004) J Alloys Compd 165:197
19. Krishnaveni K, Sankara Narayanan TSN, Seshadri SK (2005) Surf Coat Technol 190:115
20. Krishnaveni K, Sankara Narayanan TSN, Seshadri SK (2008) J Alloys Compd 466:412
21. Wu X, Sha W (2008) Appl Surf Sci (in press). doi:10.1016/j.apsusc.2008.08.018
22. Bozzini B, Martini C, Cavallotti PL, Lanzoni E (1999) Wear 225–229:806
23. McCormack AG, Pomeroy MJ, Cunnane VJ (2003) J Electrochem Soc 150(5):C356
24. Carac G, Benea L, Iticescu C, Lampke T, Steinhauser S, Wielage B (2004) Surf Eng 20(5):353
25. Qu NS, Zhu D, Chan KC (2006) Scr Mater 54:1421
26. Keong KG, Sha W, Malinov S (2003) Surf Coat Technol 168:263
27. Hollomon JH, Jaffe LD (1945) Trans AIME 162:223
28. Bhadeshia HKDH (1997) Mater Sci Eng A 223:64
29. Baloch MM, Bhadeshia HKDH (1990) Mater Sci Technol 6:1236
30. Yang Y, Torrance AA, Rodriguez J (1996) Sol Energy Mater Sol Cells 40(2):103
31. Ashby MF, Easterling KE (1982) Acta Metall 30(11):1969
32. Staia MH, Castillo EJ, Puchi ES, Lewis DB, Hintermann HE (1996) Surf Coat Technol 86–87:598
33. Wu YC, Li GH, Zhang L (2000) Surf Eng 16:506
34. Hou KH, Ger MD, Wang LM, Ke ST (2002) Wear 253:994
35. Wu G, Li N, Zhou D, Mitsuo K (2003) Surf Coat Technol 176:157
36. Chang LM, An MZ, Shi SY (2006) Mater Chem Phys 100:395
37. Grosjean A, Rezrazi M, Takadoum J, Berçot P (2001) Surf Coat Technol 137:92
38. Panagopoulos CN, Agathocleous PE, Papachristos VD, Michaelides A (2000) Surf Coat Technol 123:62
39. Panagopoulos CN, Georgarakis KG, Agathocleous PE (2003) Tribol Int 36:619